Dihydroorotate Dehydrogenase B of *Enterococcus faecalis.* Characterization and Insights into Chemical Mechanism

Jovita Marcinkeviciene,*,‡ Lisa M.Tinney,‡ Kathy H. Wang,§ M. John Rogers,§ and Robert A. Copeland‡

Department of Chemical Enzymology and Antimicrobial Group, DuPont Pharmaceuticals, P.O. Box 80400, Wilmington, Delaware 19880-0400

Received March 23, 1999; Revised Manuscript Received July 9, 1999

ABSTRACT: *Enterococcus faecalis* dihydroorotate dehydrogenase B is a heterodimer of 28 and 33 kDa encoded by the *pyrK* and *pyrDb* genes. Both subunits copurify during all chromatographic steps, and, as determined by HPLC, one FMN and one FAD are bound per heterodimer. The enzyme catalyzes efficient oxidation of 4-*S*-NADH by orotate. Isotope effect and pH data suggest that reduction of flavin by NADH at the PyrK site is only partially rate limiting with no kinetically significant proton transfer occurring in the reductive half-reaction; therefore, a group exhibiting a p*K* of 5.7 ± 0.2 represents a residue involved in binding of NADH rather than in catalysis. The reducing equivalents are shuttled between the NADH-oxidizing flavin in PyrK and the orotate-reacting flavin in PyrDb, by iron−sulfur centers through flavin semiquinones as intermediates. A solvent kinetic isotope effect of 2.5 ± 0.2 on V is indicative of rate-limiting protonation in the oxidative half-reaction and most likely reflects the interaction between the isoalloxazine N1 of the orotate-reducing flavin and Lys 168 (by analogy with *L. lactis* DHODase A). The oxidative half-reaction is facilitated by deprotonation of the group(s) with p*K*(s) of 5.8−6.3 and reflects either deprotonation of the reduced flavin or binding of orotate; this step is followed by hydride transfer to C6 and general acid-assisted protonation (p*K* of 9.1 ± 0.2) at C5 of the product.

Dihydroorotate dehydrogenase (EC 1.3.3.1) catalyzes one of the six consecutive enzymatic reactions in the de novo biosynthesis of UMP. While salvage pathways for pyrimidine nucleotides have been identified in the majority of eukaryotes and prokaryotes, highly proliferating cells require a rich supply of nucleic acids; hence, the de novo pathway is critical. Recent strategies for developing antiproliferative, antiparasitic, and immunosuppressive drugs have focused on this pathway, and mainly on dihydroorotate dehydrogenase (DHODase),[1] as a potential target enzyme (*1*−*4*). A number of mammalian and protozoan DHODases have been purified and characterized (*5*−*8*). These enzymes are membrane-associated proteins which employ FMN as a cofactor for oxidative electron transfer between dihydroorotate and the components of the respiratory chain. Studies of the desaturation process catalyzed by the *Crithidia fasciculata* (*9*) and bovine (*10*) DHODases using deuterated dihydroorotate suggested that catalysis occurred by active site base-mediated C5-*S* proton abstraction with concomitant (or subsequent) C6 hydride transfer to the N5 position of the isoalloxazine ring of FMN.

Much less mechanistic information is available on the prokaryotic dihydroorotate dehydrogenases. Besides being highly diverse in amino acid sequence, the bacterial enzymes bear little similarity to their eukaryotic counterpartners. The dihydroorotate dehydrogenases of Gram-negative bacteria are more like the eukaryotic enzymes since they are membrane-associated, despite their lack of highly hydrophobic regions large enough to span the membrane bilayer (*11*). The Gram-positive bacterium *Lactococcus lactis* (*12*) is unique in being the only organism known to contain two functional dihydroorotate dehydrogenases (referred to as A and B) encoded by separate genes within its genome. A three-dimensional crystal structure (*13*, *14*) and site-directed mutagenesis studies (*15*) of *L. lactis* DHODase A have shed light on the catalytic functionalities of the enzyme, although detailed chemical and kinetic mechanisms are still to be elucidated.

In this paper we report the sequencing of the *pyrK* gene and cloning of the complete *pyrK/pyrDb* genes of the human pathogen *Enterococcus faecalis* which encode a soluble heterotetramer protein having ∼70% similarity to *Lactococcus lactis* DHODase B enzyme. A high-yield purification scheme provided us with sufficient quantities of the protein for characterization and mechanistic studies. The combination of pH and kinetic isotope experiments has allowed us to propose a minimal chemical mechanism which incorporates acid−base catalysis employed by the enzyme.

MATERIALS AND METHODS

Cloning of the pyrK/pyrDb Genes. The sequence of the *Enterococcus faecalis pyrD* gene has been reported (*16*), and based on comparative sequence analysis with other DHODases, it was expected that the *pyrD* gene of *E. faecalis* encodes the enzymatic portion of DHODase B. A partial sequence of the enterococcal *pyrK* open reading frame (*16*)

* To whom correspondence should be addressed.
‡ Department of Chemical Enzymology.
§ Antimicrobial Group.

[1] Abbreviations: DHODase, dihydroorotate dehydrogenase; DHO, dihydroorotate; DCIP, 2,6-dichloroindophenol; NBT, *p*-nitro blue tetrazolium; KIE, kinetic isotope effect, *pyrK* and *pyrDb*, genes encoding PyrK and PyrDb subunits of the DHODase B.

10.1021/bi990674q CCC: $18.00
Published on Web 09/14/1999

was used as a basis for cloning and sequencing the complete *pyrK* gene. Genomic DNA from *E. faecalis* ATCC strain 29212 served as a template for PCR amplification and cloning. Conditions for amplification were as described for the Elongase reaction kit (Life Technologies, Gaithersburg, MD), for long-range PCR (*17*). Oligonucleotides for the initial inverse PCR reactions were designed based on GenBank entry U24692. Amplification by inverse PCR of a *Bcl*I digest of *E. faecalis* genomic DNA employed the following oligonucleotide pairs: EF1 (CATACCATTCGCACCGCAAGC)/EF2 (GGCCTGTGGAATTGGGGC) and EF3 (CCTCACTTGCTTTAAAAATCGGACC)/EF4 (CCCCGCCAGTGGTTGCTTTGGG).

Amplification from an *Apo*I digest *of E. faecalis* genomic DNA was performed using the following oligonucleotide pair: EFS6 (TCCAGCGCCTTCGACTCGAT)/EFS7 (GAGGCTGCTTATTACCAAC).

Inverse PCR products were purified and cloned into the pCR2.1 cloning vector described by the manufacturer (Invitrogen, Carlsbad, CA). Automated DNA sequence analysis was performed with an ABI 377XL DNA Sequencer (Perkin-Elmer, Foster City, CA) in the reactions using Big Dye Terminator Reaction Mix. Sequence analysis was performed with Lasergene Software (DNASTAR, Madison, WI). The complete *pyrK/pyrDb* gene was amplified and cloned as an *Xba*I/*Xho*I fragment in the corresponding sites of the polylinker of a pET15b expression vector (Novagen, Madison) using the following pair of oligonucleotides: (*Xba*I boldface) CATG**TCTAGA**AAATCATTTATAGGGGAATC; (*Xho*I boldface) CTAG**CTCGAG**AATCTAACGCAATAATTGGTCTA.

For routine cloning, *E. coli* strain DH5α was used, while the overexpression vector was transformed into the TAP330 *E. coli* strain (*8*), containing a disrupted *pyrD* gene.

Transformed cells were grown in a high-density fermentor to an OD of 20, induced with 1 mM IPTG, and incubated for an additional 3 h at 37 °C.

Purification of the Enzymes. Both subunits (PyrK/PyrDb) copurified during all chromatographic steps. Cell paste (∼50 g) was resuspended (50% w/v) in 50 mM TEA buffer containing 0.2 mg/mL lysozyme and protease inhibitor cocktail (Boehringer Mannheim, #1836170). Cells were broken by sonication, and cell debris were removed by centrifugation for 45 min at 19000*g*. All the activity was recovered in the supernatant. Nucleic acid precipitation with streptomycin sulfate (1% w/v) was followed by slow saturation with ammonium sulfate (final concentration 1.5 M), and the cloudy solution was clarified by one more centrifugation (at 19000*g* for 45 min). All of the DHODase activity was retained in the soluble fraction. This supernatant was applied to a 120 mL Phenyl Sepharose (Pharmacia) column, preequilibrated with 50 mM TEA buffer, pH 7.8, containing 1.5 M ammonium sulfate. Adsorbed protein was recovered with a linear 1.5−0 M ammonium sulfate reverse gradient. Active fractions eluting at the very end of the run (in the absence of ammonium sulfate) were pooled and loaded on a 50 mL Sepharose Q (HP, Pharmacia) anion-exchange column, equilibrated in 50 mM TEA buffer with 1% (v/v) glycerol. The activity eluted between 0.1 and 0.3 M NaCl using a 500 mL nonlinear 0−1 M NaCl gradient. Active fractions were concentrated (using an Amicon YM10 filter) to 5 mL and applied to an S-200 (Pharmacia) gel filtration column preequilibrated in 50 mM TEA with 0.2 M NaCl. Active fractions, exhibiting only two bands (corresponding to the heterodimer 28 and 33 kDa subunits) on SDS−PAGE with Coomassie blue staining, were pooled and stored in 50% (v/v) glycerol at −20 °C. The final yield of purified protein from 55.6 g of cells was 115 mg.

Determination of Flavin Content. The identity of flavin cofactors was determined using HPLC reversed-phase chromatography. An enzyme solution was diluted (50% v/v) in the elution buffer (described below), boiled for 5 min, filtered through a YM10 ultrafiltration membrane (Amicon), and injected onto a C18 Bondpack column (3.9 × 150 mm, Waters). The column was developed isocratically with 20% methanol containing 0.5 mM ammonium acetate and 0.1% TFA (*18*). Calibration curves were made with commercially available FMN and FAD (Fluka) cofactors (0.1−1 nmol).

Determination of Inorganic Iron. Iron content was determined as described by Nielsen et al. (*19*). Enzyme (5−20 nmol) was precipitated with TCA. After adjustment of the pH to 4.5 with ammonium acetate, the supernatant was reacted with hydroxylamine hydrochloride and tripyridyl-*s*-triazine (Sigma), and absorbance spectra were recorded. The peak at 595 nm was quantified using a calibration curve obtained with $FeCl_3 \cdot 6H_2O$ (1 nmol of iron gave an absorbance of 0.0144).

Enzyme Concentration Determination. The enzyme concentration was quantitated using three independent methods: Bradford total protein concentration; flavin absorbance at 452 nm [considering that FAD has an extinction coefficient of 11 300 M^{-1} cm^{-1} (*20*) and FMN has an extinction coefficient of 12 200 M^{-1} cm^{-1} (*5*)]; and change in tyrosinate absorbance at alkaline pH (*21*).

Spectrophotometric Titrations. A 10−17 μM enzyme solution was made anaerobic by several cycles of evacuation and filling with oxygen-free nitrogen. Substrate solutions (DHO or NADH) were prepared in an analogous way in a separate rubber-stopper tightened vial and introduced into the cuvette using a gastight syringe. Spectra were recorded with a Cary 50 spectrophotometer (Varian).

Enzyme Assays. Four enzymatic assays were used in this study. The assay employed during purification was based on the reduction of NBT in the presence of 0.1 mM DHO and was performed in a 96 well plate (*8*). The 0.2 mL reaction mixture typically contained 0.1 M Tris buffer, pH 7.5, with 0.1% Triton X-100 (to solubilize the product: NBT formazan) and a defined amount of the active fraction. The reaction was initiated by adding DHO. The extinction coefficient of formazan [12.3 mM^{-1} cm^{-1} (*22*)] was corrected for the plate well path length using a calibration curve of known concentration solutions and measuring the absorbance both in a 1 cm cuvette and in a 0.2 mL well. All other assays were performed in 1 cm path length cuvettes.

The second assay was based on orotate absorbance at 278 nm (ϵ = 6.7 mM^{-1} cm^{-1}). The assay mixture contained variable amounts of DHO and 50 μM DCIP as the electron acceptor in 0.1 M Tris buffer, pH 7.5. The reaction was monitored at 278 nm, following the orotate production.

The last two assays monitored either oxidation of NADH or reduction of NAD^+ at 340 nm (ϵ = 6.2 mM^{-1} cm^{-1}) in 0.1 M Tris buffer, pH 7.5, in the presence of orotate or DHO, respectively. The transhydrogenation reaction was performed

under anaerobic conditions monitoring the reduction of thio-NAD^+ at 395 nm ($\epsilon = 11.3\ mM^{-1}\ cm^{-1}$).

pH Profiles. The following buffers (0.1 M) were prepared and used for the identification of ionizable groups: MES, pH 5.5−6.5; phosphate, pH 6.5−7.5; TRIS, pH 7.5−8.5; carbonate, pH 8.5−9.5. Overlapping points were used to ensure the absence of specific buffer effects on enzyme activity.

Preparation of (4S)- and (4R)-Labeled Reduced Pyridine Nucleotides. [4*S*-4-^{1}H]- and [4*S*-4-^{2}H]-NADH were synthesized using NAD^+ and 1-protio- or 1-deuterioglucose (Sigma) as starting materials in the presence of ATP, $MgCl_2$, hexokinase (3.2 units), and glucose-6-phosphate dehydrogenase (3 units). The reaction was allowed to go to completion (∼1 h at 37 °C), and the products were purified on a MonoQ anion exchange column (Pharmacia), as described previously (*23*). Fractions exhibiting $A_{260}/A_{340} < 2.3$ were pooled and used for further experiments. [4*R*-4-^{1}H]- and [4*R*-4-^{2}H]-NADH were synthesized using protio- and deuterioethyl alcohol in the presence of alcohol dehydrogenase (5 units) (Sigma). The reaction products were purified as described above. Deuterium incorporation into [4*S*-4-^{2}H]-NADH was 95% complete, as determined by ^{1}H NMR spectroscopy.

Solvent Kinetic Isotope Effects. Ten times concentrated (10×) reaction mixtures, excluding the variable substrate, were prepared in 10× buffer solution and then diluted either with D_2O (Fluka, 99.95% purity) or with H_2O; final D_2O solutions were considered to have 90% of the label. The variable substrate was prepared separately either in D_2O or in H_2O and added to the reaction mixture to initiate the reaction.

Alkylation Studies. Solutions of DHODase B (4.6 μM) at different pHs (0.1 M Tris, pH 7.5−9.7) were preincubated with 1 mM iodoacetamide. Aliquots were taken at different time points, and the remaining activity was measured in the DHO−DCIP assay, following orotate production.

Data Analysis. The data were fit to the appropriate equations using either Cleland's programs (*24*) or SigmaPlot software. The individual saturation curves for the K_m and V determinations were fit to eq 1. Data for pH profiles decreasing at low and high pH values with slopes of +1 and −1 were fit to eq 2. The data for the pH profile decreasing with a slope of −1 at low pH values were fit to eq 3, while the data increasing with a slope of 1 at high pH values were fit to eq 4. The primary kinetic isotope data, assuming an effect on V only, were fit to eq 5, while data for which isotopic substitution affected both V and V/K were fit to eq 6. Equation 7 describes the data for which a kinetic isotope effect was observed on V/K only.

$$v = VA/(K + A) \quad (1)$$

$$y = C/(1 + H/K_a + K_b/H) \quad (2)$$

$$y = C/(1 + H/K) \quad (3)$$

$$y = C(1 + H/K)/H \quad (4)$$

$$v = VA/[K + A(1 + F_iE_V)] \quad (5)$$

$$v = VA/[K(1 + F_iE_{V/K}) + A(1 + F_iE_V)] \quad (6)$$

$$v = VA/[K(1 + F_iE_{V/K}) + A] \quad (7)$$

In all equations, A is the concentration of the variable substrate, y is the experimental value of the parameter at a given pH, C is the pH-independent value of y, K_a and K_b are dissociation constants for the ionazable groups, F_i is the fraction of deuterium in the labeled substrate, and E_V and $E_{V/K}$ are isotope effects minus 1. The interpretation of the data was made using expressions for the kinetic isotope effects on V/K and V for a ping-pong kinetic scheme as derived by Vanoni et al. (*25*).

RESULTS

Expression and Purification of the E. faecalis pyrK/pyrDb Proteins. The sequence of the gene encoding the PyrDb protein has been published (*16*), and by analogy with the *Lactococcus lactis* gene organization, we predicted that the sequence upstream should encode the PyrK subunit of DHODase B. The termination codon of *pyrK* was found to overlap with the ATG codon of *pyrDb* (nucleotide 226 in GenBank entry U24692). To obtain the complete *pyrK* gene, additional sequence was obtained by inverse PCR. Cloning and sequencing the PCR product showed that it was missing about 60 amino acids of the complete *pyrK* gene. The complete *pyrK* ORF of 263 amino acids was then obtained from inverse PCR with an *Apo*I digest of genomic DNA; the sequence of the protein encoded by the *pyrK* gene is shown in Figure 1. The predicted molecular masses of the *pyrK* and *pyrDb* gene products are 28.5 and 32.9 kDa, respectively. These molecular masses were confirmed by electrospray mass spectrometry after the proteins were purified to electrophoretic homogeneity (Figure 2). The molecular mass determined by gel filtration was approximately 125 000 Da, suggesting that the native enzyme exists as a heterotetramer.

Cofactor Analysis. The presence of two flavin cofactors was anticipated by analogy with *Lactococcus lactis* DHODase B (*19*): FAD being a cofactor in the PyrK subunit and FMN binding to the PyrDb. Both cofactors were released from the apoproteins by boiling and were separated on an analytical HPLC reversed phase column with retention times of 3.51 and 5.16 min for FAD and FMN, respectively. The stoichiometry calculated from the standard calibration curve with commercial coenzymes confirmed that 1 mol of each cofactor was bound per mole of heterodimer. The brownish color (absorbance at ∼550 nm) of the enzyme solution and the cysteine-rich domain at the C-terminus of the PyrK subunit suggested the presence of nonheme iron, most likely in iron−sulfur clusters (*26*, *27*). The inorganic iron content was quantified by the method described earlier (*19*), and a value of 1.75 ± 0.50 atoms of Fe per mole of enzyme has been estimated. Presumably, the iron is present in [2Fe-2S] redox centers (as has been reported for the lactococcal enzyme), although a more detailed analysis would be needed to confirm this assignment.

Substrate Specificity and Spectrophotometric Titration. Enterococcus faecalis DHODase B catalyzed the oxidation of L-dihydroorotate using NBT, DCIP, and molecular oxygen as electron acceptors. None of these reactions were activated by the presence of coenzyme Q_6, suggesting that an alternative physiological electron acceptor should exist for this enzyme. NAD^+ was even less effective as a substrate than were the synthetic dyes with dihydroorotate. NADH (but not

```
B. caldolyticus  M.IGRERMTV ASQRLIAERT YELTLSGRLV QEMRQPGQFV HVKVAASADP
B. subtilis      M..KKAYLTV CSNQQIADRV FQMVLKGELV QGFTTPGQFL HLKVSEAVTP
E. faecalis      MQRKQEMMTI VAQKQLAPRI YQLDLQGELV KEMTRPGQFV HIKVPRA.DL
L. lactis        MSQLQEMMTV VSQREVAYNI FEMVLKGTLV DEMDLPGQFL HLAVPNGA.M
Consensus        M--KQEMMTV VSQRQIA-RI ---VLKGELV QEMT-PGQF- HLKVP-AADP

                 51                                                  100
B. caldolyticus  LLRRPLSLCH IDHKQGQCTI IYRQ..EGKG TALLAQKQPG DTVDVLGPLG
B. subtilis      LLRRPISIAD VNFEKNEVTI IYRV..DGEG TRLLSLKQQG ELVDVLGPLG
E. faecalis      LLRRPISINQ IDHSNETCRL IYRV..EGAG TEVFATMKAG EQLDILGPLG
L. lactis        LLRRPISISS WDKRAKTCTI LYRIGDETTG TYKLSKLESG AKVDVMGPLG
Consensus        LLRRPISI-- IDH---TCTI IYRV--EG-G T-LL--KQ-G E-VDVLGPLG

                 101                                                 150
B. caldolyticus  NGFPLEAAPA GSRALLVGGG IGVPPLYELA KQLTKRGVKV VSVLGFQTKA
B. subtilis      NGFPVNEVQP GKTALLVGGG VGVPPLQELS KRLIEKGVNV IHVLGFQSAK
E. faecalis      NGFDITTVAA GQTAFIVGGG IGIPPLYELS KQLNEKGVKV IHFLGYASKE
L. lactis        NGFPVAEVTS TDKILIIGGG IGVPPLYELA KQLEKTGCQM TILLGFASEN
Consensus        NGFPV-EV-A G-TAL-VGGG IGVPPLYEL- KQL--KGVKV IHVLGF-SK-

                 151                                                 200
B. caldolyticus  AVFYEEEFAA FGET..HVAT DDGS...HGT AGRVTDVIEA RSLEFDVLYA
B. subtilis      DVFYEEECRQ YGDT..YVAT ADGS...YGE TGFVTDVIKR KKLEFDILLS
E. faecalis      AAYYQQEFMA LGET..HFAT DDGSFGAHGN VGRLLSEALA KGRIPDAVYA
L. lactis        VKILENEFSN LKNVTLKIAT DDGSYGTKGH VGMLMNEI.. .DFEVDALYT
Consensus        AVFYEEEF-A LGET--HVAT DDGS-G-HG- VGR-TD-I-A K-LEFDALYA

                 201                                                 250
B. caldolyticus  CGPKPMLRAL AERFP.NRPV YLSLEERMGC GVGACFACVC HVPGSETAYK
B. subtilis      CGPTPMLKAL KQEYA.HKEV YLSMEERMGC GIGACFACVC HTNESETSYV
E. faecalis      CGANGMLKAI DSLFPTHPHV YLSLEERMAC GIGACYACVC HKKGDTTGAK
L. lactis        CGAPAMLKAV AKKYDQLERL YISMESRMAC GIGACYACVE HDKEDES..H
Consensus        CG--PMLKAL A---P-H--V YLS-EERM-C GIGAC-ACVC H-K--ET-YK

                 251             268
B. caldolyticus  ..KVCSDGPV FRAGEVVL
B. subtilis      ..KVCLDGPV FKAQEVAL
E. faecalis      SVKVCDEGPI FKASEVIL
L. lactis        ALKVCEDGPV FLGKQLSL
Consensus        --KVC-DGPV FKA-EV-L
```

FIGURE 1: Amino acid sequences of the *Bacillus caldolyticus*, *Bacillus subtilis*, *Lactococcus lactis*, and *Enterococcus faecalis* PyrK proteins.

NADPH), however, was rather efficiently oxidized in the presence of orotate (Table 1). The kinetic parameters for these three reactions catalyzed by *E. faecalis* DHODase B are summarized in Table 1. This ability to catalyze a faster reverse than forward reaction is not without precedent since a "catabolic" DHODase, functioning as an NADH-dependent orotate reductase, has been isolated from *Clostridium oroticum* grown on orotate as a carbon source (*28*). *E. faecalis* DHODase B catalyzed reduction of orotate follows a steady-state ping-pong kinetic mechanism, as determined by the series of parallel lines observed when reciprocal velocities were plotted against the reciprocal orotate concentrations at various fixed NADH concentrations (Figure 3).

The presence of two different flavin cofactors suggests their nonequivalency in catalysis. The reactivity of enzyme flavins with sulfite has been exploited by several investigators to differentiate the coenzyme environments in flavoenzymes (*29*−*31*). Anaerobic titration of the enzyme with 0.1−10 mM sodium sulfite resulted in a modest change of the flavin spectrum (traces 1 and 2 in Figure 4A). The rapid reduction of one flavin (decrease of ∼50% in total absorbance at 450 nm) by 0.1 mM NADH was not affected by the presence of sulfite. The spectrum did not change with time, and the addition of 1 more equiv of NADH resulted in very little change in absorbance. These data suggest that the flavin cofactor oxidizing NADH is not reactive with sulfite. On the other hand, when a new aliquot of anaerobic enzyme solution was treated with 10 mM sulfite and subsequently reduced with 0.1 mM dihydroorotate, a gradual decrease in the 450 nm absorbance with time was observed. The time interval between spectra (Figure 4B) was 2 min, indicating that the reduction of flavin at the dihydroorotate oxidation site is slow. Pre-steady-state experiments (data not shown) determined that the reduction of flavin by DHO occurs at a rate of 73.6 ± 6.9 s^{-1} (20 μM enzyme and 40 μM DHO at 25 °C), suggesting that the slow rate observed in spectrophotometric titration studies is due to the displacement of sulfite by DHO. A similar insensitivity of the flavin to sulfite at the NADPH oxidizing site (FAD) has been observed for glutamate synthase, while the reaction at the imine reduction site (FMN) was reversibly perturbed by sulfite (*31*).

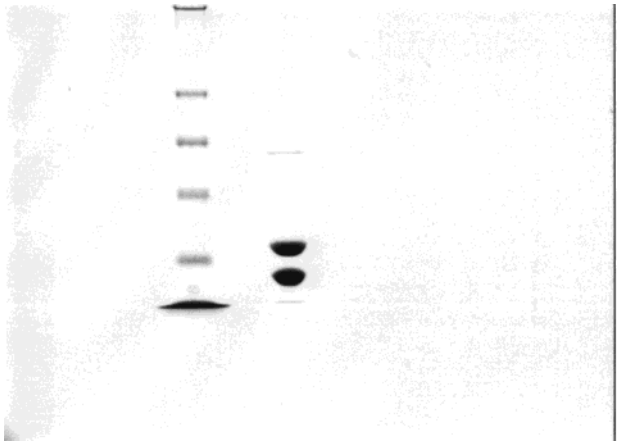

FIGURE 2: SDS−PAGE of the purified *E. faecalis* DHODase B (PyrK/PyrDb). Lane 1, molecular weight markers; lane 2, purified protein.

Table 1: Reactions Catalyzed by *Enterococcus faecalis* DHODase B in 0.1 M Tris, pH 7.5, 0.1 mM Fixed Substrate

reaction	K_m (μM)	k_{cat} (s^{-1})	k_{cat}/K_m ($\times 10^5$ M^{-1} s^{-1})
NADH + orotate	36.4 ± 2 (for orotate) 27.0 ± 3.1 (for NADH)	18.0 ± 0.2	5.5 ± 1.2
NAD^+ + DHO	33.2 ± 4.1 (for DHO) 135 ± 18 (for NAD^+)	0.4 ± 0.1	0.12 ± 0.04
NBT + DHO	27.6 ± 1.2 (for DHO)	1.04 ± 0.2	0.38 ± 0.03

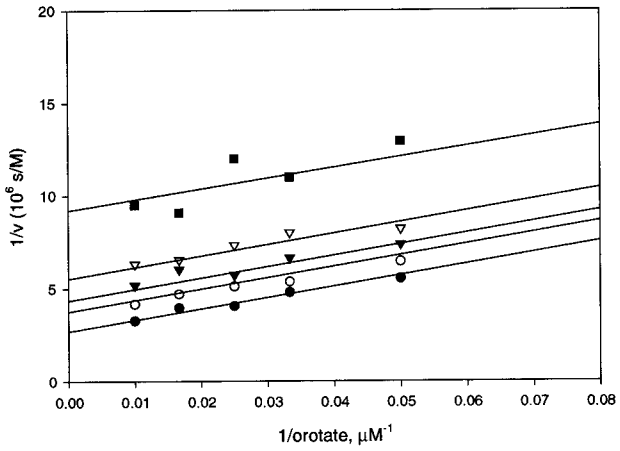

FIGURE 3: Initial velocity pattern for orotate reduction catalyzed by *E. faecalis* DHODase B at 100, 40, 30, 20, and 10 μM NADH in 0.1 M Tris buffer, pH 7.5.

Effect of pH on the Kinetic Parameters of the NADH−Orotate Reaction. The pH profiles for the kinetic parameters of the *E. faecalis* DHODase catalyzed reaction were obtained when orotate was varied between 0.01 and 0.1 mM in the presence of 0.1 mM NADH (Figure 5A) or when NADH was varied between 0.01 and 0.1 mM in the presence of 0.1 mM orotate (Figure 5B) at pH values between 5.9 and 9.8. As is predicted for a ping-pong kinetic mechanism, V/K for the variable substrate did not change with the concentration of saturable substrate. The maximum velocity (V) dependence on pH for both reactions is shown in Figure 5C. The $V/K_{orotate}$ profile shows a decrease in activity at low and high pH

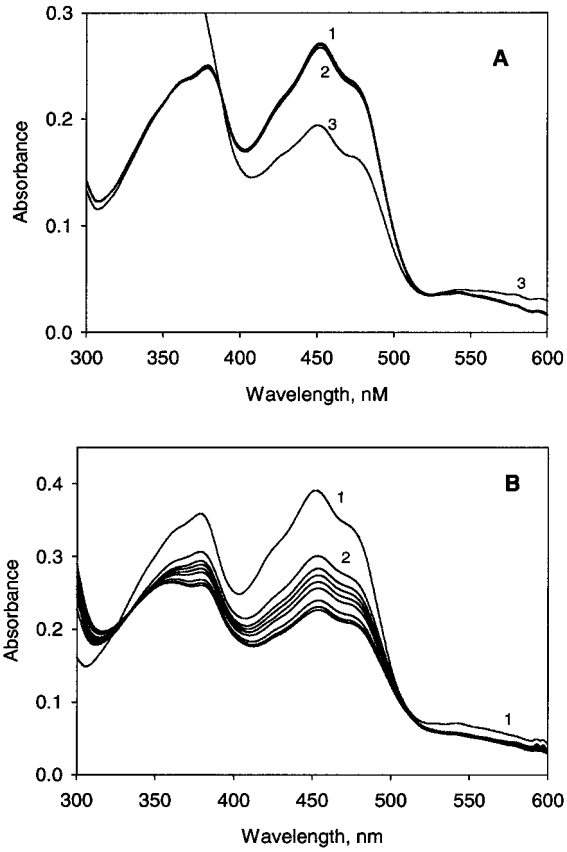

FIGURE 4: Spectrophotometric titration of *E. faecalis* DHODase B (13−17 μM). (A) Traces 1 and 2, titration with 0.1, 1, and 10 mM sulfite; trace 3, with addition of 0.1 mM NADH. (B) Trace 1, enzyme with 10 mM sulfite; traces 2−9, at various times after addition of 0.1 mM DHO. Spectra in traces 2−9 were taken at 2 min intervals.

values, when groups with pK values of 6.3 ± 0.2 and 9.3 ± 0.2 are protonated and deprotonated, respectively (Figure 5A). V/K_{NADH} decreases at low pH as a single group with a pK value of 5.7 ± 0.2 is protonated (Figure 5B). The maximum velocity profile is pH-independent between pH 6 and 8, and protonation of an acidic group and/or deprotonation of an alkaline residue results in the decrease of V.

Primary Substrate Deuterium and Solvent Kinetic Isotope Effects. Primary deuterium kinetic isotope effect studies with [4*S*-4-^{1}H]-NADH, [4*S*-4-^{2}H]-NADH, [4*R*-4-^{1}H]-NADH, and [4*R*-4-^{2}H]-NADH at pH 7.5 revealed that the enzyme catalyzes stereospecific *pro-S* C4 hydrogen abstraction from NADH, since no kinetic isotope effect was observed when the *pro-R*-deuterated substrate was used. A small, but statistically significant $^DV/K_{NADH}$ of 1.42 ± 0.08 is obtained from fitting the data to eq 7. The best fit was chosen primarily on the basis of visual inspection of the experimental data, and then calculating the fits and evaluating the lowest values of the standard error of the kinetic parameter. Solvent kinetic isotope effects, using NADH as the variable substrate, were performed in 90% D_2O solution in the pH-independent region. Only the intercepts of reciprocal plots were affected by the isotopic composition, suggesting that no protons are being transferred during the reductive half-reaction. Surprisingly, the same pattern of plots was obtained using orotate as the variable substrate; the calculated ^{D2O}V was 2.7 ± 0.3 (Table 2), which suggests that potentially there is a kinetically significant proton transfer in the rate-limiting step. Since

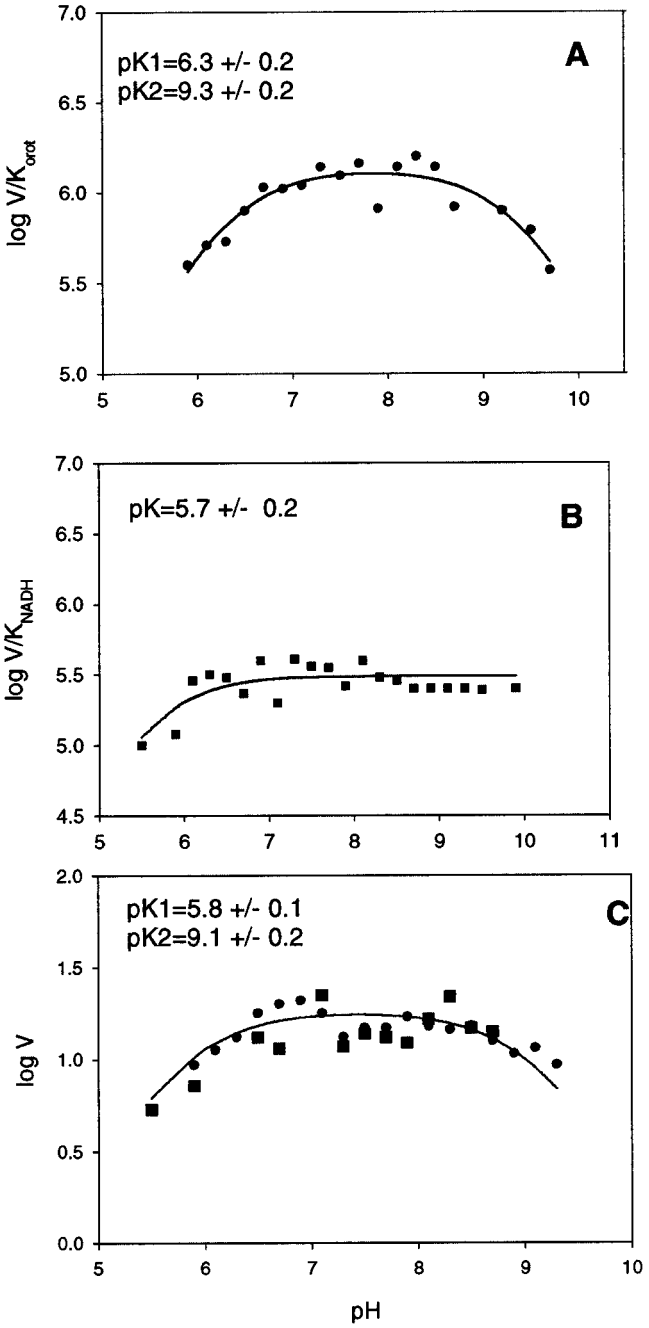

FIGURE 5: Effect of pH on the kinetic parameters for the NADH−orotate reaction catalyzed by *E. faecalis* DHODase B. (A) (●) Data collected varying orotate at 0.1 mM NADH; (B) (■) data collected varying NADH at 0.1 mM orotate; (C) data collected varying orotate (●) and NADH (■).

dihydroorotate oxidation catalyzed by bovine and *Crithidia fasciculata* DHODases (*9*, *10*) involves solvent-exchangeable proton abstraction, similar proton transfers were expected in the reaction catalyzed by *E. faecalis* DHODase. To clarify this situation, we followed the DCIP-mediated oxidation of DHO at 278 nm (orotate production) in both H_2O and D_2O solutions (the pH profiles of the parameters for this reaction were pH-independent above pH 7.4; data not shown). An inverse kinetic solvent isotope effect of 0.63 ± 0.15 was observed in this reaction for V/K_{DHO}, while the ^{D2O}V value was the same as in the experiments described earlier (Table 2).

DISCUSSION

The discovery of two structurally diverse, functional DHODase enzymes in *Lactococcus lactis* (*12*) suggested that similar functionalities might exist in other Gram-positive bacteria. We focused our attention on the human pathogen *Enterococcus faecalis* because of the importance of this microorganism from a clinical perspective. *Enterococcus faecalis* is a causative agent in a number of clinical infectious diseases including subacute bacterial endocarditis (*32*). Human DHODase has proved to be a useful therapeutic target for attenuating immune cell proliferation (*3*). By analogy, the bacterial DHODases are potential targets for therapeutic intervention as well, though the paucity of mechanistic information concerning bacterial DHODases is, however, a hindrance to rational inhibitor design. This has encouraged us to undertake the complete sequencing of the genes encoding enterococcal DHODase B and to characterize the product of these genes by elucidating the critical steps in catalysis.

The presence of a heterotetrameric soluble DHODase, encoded by two different genes, is not without precedence for Gram-positive bacteria. Along with *Lactococcus lactis*, two open reading frames putatively corresponding to *pyrK* and *pyrDb* were identified in *Bacillus subtilis* (*33*). The amino acid sequences of the subunits we have cloned from *Entrococcus faecalis* are 41.4% and 71.2% similar to the *L. lactis* PyrK/PyrDb subunits, respectively, and 44.5% and 61.4% to the PyrDII and PyrDI proteins of *B. subtilis*. The purification and characterization of the *E. faecalis* PyrK/PyrDb enzyme support the initial hypothesis that the enzyme shares numerous structural and catalytic features with the soluble type B DHODases from other Gram-positive bacteria.

The diversity of the chemical reactivity of the flavin coenzymes, determined by their structure, renders them highly versatile cofactors with considerable efficiency in a wide variety of enzymatic reactions involving either one- or two-electron transfers. Because of this versatility, flavins often serve as transformation sites between obligate two-electron and one-electron donors/acceptors. This property is obviously under strict control of the surrounding protein moiety.

The identification of two distinct active site flavins has been proven for a number of enzymes (*29*, *31*). In addition to selective reactivity with substrates, flavins can be distinguished in model reactions according to their reactivity with sulfite. Massey and Hemmerich (*30*) described the correlation between the ability of a particular flavoprotein to stabilize a red anion radical and the ease of sulfite addition to the N5 position of the isoalloxazine. The proximity of a protonated base of the protein to the N1 position of the flavin would facilitate the nucleophilic addition of sulfite to the N5 position. A refined three-dimensional structure, at 2 Å resolution, of *L. lactis* DHODase A revealed that Lys164 is hydrogen-bonded to the N1 of the FMN isoalloxazine ring (*13*). This residue is conserved in the aligned *E. faecalis* PyrDb sequence (Lys 168), potentially explaining the sensitivity of the orotate active site flavin (FMN) to sulfite. In contrast, the reduction of the enzyme with NADH resulted in a slight increase of absorbance at ~600 nm (Figure 4A), indicative of a neutral flavin radical. This spectral feature is usually not accompanied by sulfite reactivity.

Table 2: Summary of the Primary Kinetic Isotope Effects of the Reactions Catalyzed by *E. faecalis* DHODase B

	substrate kinetic isotope effect		solvent kinetic isotope effect		
reaction	$^{D}V/K_{NADH}$	^{D}V	$^{D2O}V/K_{NADH}$	$^{D2O}V/K_{orot}$	^{D2O}V
NADH + orotate	1.42 ± 0.08	no effect	no effect	no effect	2.7 ± 0.3
DHO + DCIP	nd[a]	nd	nd	0.63 ± 0.15	2.5 ± 0.2

[a] nd, not determined.

Our data are in good agreement with the data reported by Singer et al. (*28*) for the clostridial enzyme where the EPR signal elicited with NADH produced a signal width of 19 G (characteristic of the neutral radical) while both 19 G and 15 G signals (anion radical) were generated upon the reduction of the enzyme with dihydroorotate.

The reactions catalyzed by *E. faecalis* DHODase B follow the two-site ping-pong kinetic mechanism (Figure 3) as expected for the two physically distinct substrate binding units. Transhydrogenation of thio-NAD^+ by NADH under anaerobic conditions was independent of orotate.

pH Profiles and Kinetic Isotope Effects. To better understand the chemical nature of the residues critical for catalysis, we investigated the pH dependence of the *V* and *V/K* values for both substrates. pH profiles for bimolecular rate constants (*V/K*) reflect the ionization behavior of groups on either substrate or free enzyme or both that affect binary complex formation.

V/K_{orot} Profile. Orotate has no titratable groups within the pH range studied, indicating that both ionizable groups observed in V/K_{orot} derive from the enzyme. The unambiguous identification of the active site base, with a p*K* of 6.3 ± 0.2, which affects either binding or reduction of orotate is complicated since no obvious acidic residues are present in the orotate binding locus. Data obtained for the homologous enzyme dihydropyrimidine dehydrogenase favor the involvement of a group exhibiting a p*K* of ~6.0 in binding rather than in catalysis, since the dissociation constant for the competitive inhibitor, 2,6-dihydroxypyridine, was still dependent upon the ionization of the same group (*34*). Structural data for lactococcal DHODase A revealed that both nitrogens of orotate make very well-defined hydrogen bonds with Asn 67 and Asn 193 (conserved as Asn 71 and Asn 195 in the *E. faecalis* DHODase B sequence), and these bonds appear to be critical for proper stacking of orotate and the flavin ring system (*14*). On the other hand, since orotate reduction is rate-limiting in the overall reaction, the group exhibiting a p*K* of 6.4 could be the same group observed in the *V*−pH profile (p*K* 5.8 ± 0.1) and hence reflect the residue involved in catalysis, most likely ionization of the N1 of FMN.

The correct protonation of the group with a p*K* of 9.3 ± 0.2 could be required for orientation and proper binding of the substrate or for the subsequent chemical step: protonation of C5 which is preceded by hydride transfer from FMN to the C6 position of orotate. In addition to four completely conserved Asn residues surrounding the substrate binding cavity in DHODase A, Lys 43 is well-conserved (as Lys 47 in *E. faecalis* DHODase B) and interacts both with orotate and with the N5 of the flavin. A K43A mutant of lactococcal DHODase A demonstrated impaired substrate binding and greatly reduced V_{max} (*15*); therefore, it is possible that the group with a p*K* of 9.3 is a conserved lysine residue.

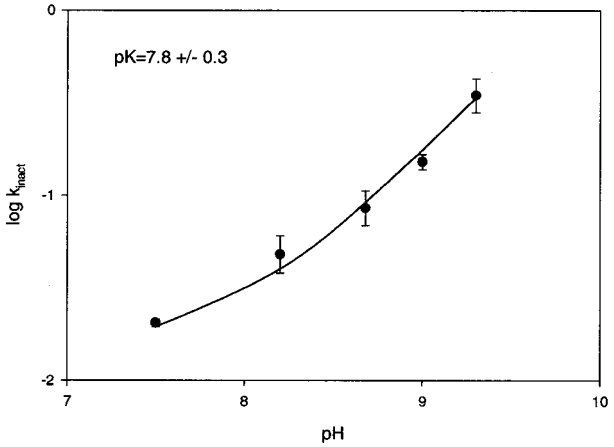

FIGURE 6: Dependence of the inactivation rate of *E. faecalis* DHODase B by iodoacetamide on pH.

On the other hand, there is evidence indicating that in dihydropyrimidine dehydrogenase a cysteine residue serves as the general acid, protonating reduced uracil (*34*−*36*). Cys 130 in *L. lactis* DHODaseA (which is conserved as Cys 133 in *E. faecalis* DHODase B) has been proposed as the active site base, abstracting the C5 proton of DHO in the oxidative half-reaction. It has been reported that the p*K* of the cysteine in *L. lactis* A enzyme is rather high (~9.0) (*14*, *15*). Our alkylation studies support the hypothesis that a cysteine residue is important in catalysis, but the calculated p*K* value of 7.8 (Figure 6) suggests that this is unlikely to be the residue accounting for the p*K* of ~9.0 in the pH profiles. The inverse solvent kinetic isotope effect of 0.63 ± 0.15 ($^{D2O}V/K_{DHO}$), measured in the DHO oxidation reaction direction catalyzed by *E. faecalis* DHODase B, is suggestive of the inverse reactant state effect attributed to thiol ionization (*37*); therefore, these results support a role for Cys 133 functioning as an active site base. No inverse solvent isotope effect on V/K_{orot} was observed in the reverse, NADH−orotate reaction, most likely indicating that the proton-transfer step before the C5 protonation of reduced orotate is rate-limiting (deprotonation of N1 of the flavin), or that Cys 133 forms an ion pair with another residue, the ionization properties of which would fulfill the requirements for catalysis.

V/K_{NADH} Profile. The interpretation of V/K_{NADH} pH profiles is speculative with respect to specific amino acid assignments since no structural information is available for the PyrK analogues, in which the NADH half-reaction occurs. A comparison can be made between dihydropyrimidine dehydrogenase and phthalate dioxygenase reductase (*38*). An active site base with a similar p*K* of 5.8 has been observed to govern the reductive half-reaction in dihydropyrimidine dehydrogenase, but lack of solvent KIE on V/K_{NADH} (which is supportive of direct hydride transfer without other kinetically significant protonations occurring in the reductive half-reaction) rules out this possibility in the case of the *E. faecalis*

DHODase B, suggesting that a group exhibiting a p*K* of 5.7 ± 0.2 is involved in NADH binding. The type II NAD binding site (*38, 39*) sequence fingerprint, consisting of glycines which define a common nucleotide phosphate binding loop, and an aspartic acid residue downstream of this sequence, is well-conserved in the *E. faecalis* PyrK subunit (D191). It has been suggested that protonation of this aspartate effects substrate binding since it forms hydrogen bonds to the adenine ribose (*38*). The moderate substrate kinetic isotope effect on V/K_{NADH} and the lack of substrate kinetic isotope effect on *V* (Table 2) are consistent with the reductive half-reaction at the FAD of the PyrK subunit being faster than the oxidative half-reaction. NADH, however, dissociates from the enzyme−nucleotide complex more rapidly than the hydride ion is transferred to FAD (*40*).

V Profile. Two enzyme ionizations are observed in the *V*−pH profile, which reflect groups involved in overall catalysis, most likely the slower oxidative half-reaction. The groups exhibiting p*K* values of 5.8 ± 0.1 and 9.1 ± 0.2 could be the same observed in the V/K_{orot} profile, conferring binding or the protonation of the product (see the discussion of *V*/*K*$_{orot}$ *Profile*). A pronounced solvent kinetic isotope effect on *V* (2.7 ± 0.3), which is observed in both reaction directions (NADH−orotate as well as DHO−DCIP), and the lack of a solvent isotope effect on V/K_{NADH} are consistent with rate-limiting proton transfer occurring in the oxidative half-reaction at the putative FMN site. Two events in this half-reaction could account for the observed solvent kinetic isotope effect, and the contribution of each of them can be evaluated by measuring the forward (NADH−orotate) and the reverse (DHO−DCIP) reactions. The rate-limiting exchange of the protium with deuterium at the reduced flavin (most likely N1 of isoalloxazine) will reflect the transition state effect that accompanies transfer of a hydride from N5 of FMN to C6 of orotate and is the main source of the solvent kinetic isotope effect observed in the forward reaction. The reverse reaction reveals the sources of both solvent kinetic isotope effects: the reactant state effect, which is inverse in the case of thiol ionization (inverse $^{D2O}V/K_{DHO}$); and the same transition state effect (^{D2O}V of 2.5 ± 0.2).

Proposed Chemical Mechanism. Based on the results outlined above, we propose a minimal chemical mechanism that attempts to account for the findings discussed in this study (Scheme 1). The binding of NADH at the putative FAD active site is followed by direct hydride transfer from the 4*S* position of the nicotinamide ring to the N5 position of the FAD isoalloxazine ring. The active site residue with a p*K* of 5.7 must be involved in binding of NADH since no solvent isotope effect was observed on V/K_{NADH}. There is suggestive, but not definitive, evidence that electrons between two active sites (FAD and FMN) are transferred by the Fe-S cluster; therefore, at least transient semiquinone forms of both flavins are anticipated. One-electron reoxidation of $FADH^-$ results in the blue semiquinone. Catalytic turnover of the second active site most likely involves red and blue semiquinones, their ratio depending upon the protonation state of Lys 168 (by analogy to the lactococcal Lys 164). Our solvent kinetic isotope studies argue that this is a slow step in the oxidative half-reaction. The oxidative half-reaction is governed by acidic group(s) with p*K* of 5.8−6.3, or N1 of FMN. On the basis of the structural and functional similarity to dihydropyrimidine dehydrogenase and *L. lactis* DHODase

Scheme 1: Proposed Minimal Chemical Mechanism for the NADH−Orotate Reaction Catalyzed by *E. faecalis* DHODase B

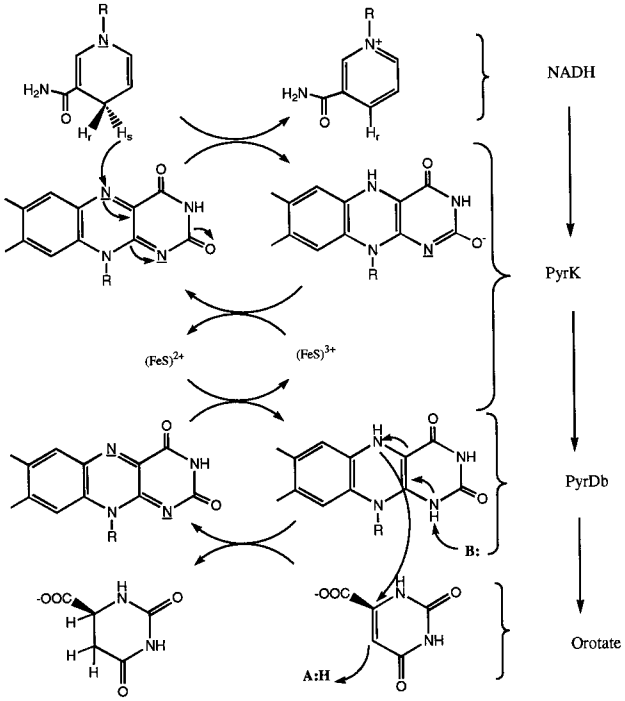

A, we propose that $FMNH_2$ directly transfers a hydride ion to the C6 of orotate, and general acid-assisted protonation at C5 yields the product, dihydroorotate.

Since mammalian dihydroorotate dehydrogenases are biosynthetic enzymes, catalyzing an important step in pyrimidine assimilation, it is tempting to speculate about the role of bacterial catabolic enzymes. Although the *E. faecalis pyrK/pyrDb* genes are found in a cluster together with the rest of the genes encoding the enzymes of the pyrimidine biosynthetic pathway, an additional alternative function of the enzyme—that of orotate catabolism—is obvious from our present studies. Since *Enterococcus faecalis* is a facultative anaerobe, we cannot exclude the possibility that, under restricted oxygen conditions, when conventional energy production is impaired, other metabolic pathways are induced that would rely on orotate catabolism. High energetic value can be obtained from carbamoyl phosphate, which is only two steps away from dihydroorotate, and it has been reported that an ATP-generating carbamate kinase is induced in *E. faecalis* under the extreme conditions (*41*).

ACKNOWLEDGMENT

We are grateful to Prof. John Blanchard, Albert Einstein College of Medicine, Dr. Dennis Murphy, Dr. Mark Harpel, Dr. Alan Rendina, and Dr. Andrew Stern for reading the manuscript and helpful discussions. We thank Karl Blom for mass spectroscopy, Jeanne I. Corman for protein sequencing results, and Stuart Rosenfeld for growing the PyrDb/PyrK-transformed *E. coli*.

REFERENCES

1. Chen, S. F., Perrella, F. W., Behrens, D. L., and Papp, L. M. (1992) *Cancer Res. 52*, 3521−3527.
2. Harder, A., and Haberkorn, A. (1989) *Parasitol. Res. 76*, 8−12.

3. Ruckermann, K., Fairbanks, L. D., Carrey, E. A., Hawrylowicz, C. M., Richards, D. F., Kirschbaum, B., and Simmonds, H. A. (1998) *J. Biol. Chem. 273*, 21682−21691.
4. Davis, J. P., Cain, G. A., Pitts, W. J., Magolda, R. L., and Copeland, R. A. (1996) *Biochemistry 35*, 1270−1273.
5. Krungkrai, J., Cerami, A., and Henderson, G. B. (1991) *Biochemistry 30*, 1934−1939.
6. Knecht, W., Altekruse, D., Rotgeri, A., Gonski, S., and Loffler, M. (1997) *Protein Expression Purif. 10*, 89−99.
7. Pascal, R. A., LeTrang, N., Cerami, A., and Walsh, C. T. (1983) *Biochemistry 22*, 171−178.
8. Copeland, R. A., Davis, J. P., Dowling, R. L., Lombardo, D., Murphy, K. B., and Patterson, T. A. (1995) *Arch. Biochem. Biophys. 323*, 79−86.
9. Pascal, R. A., and Walsh, C. T. (1984) *Biochemistry 23*, 2745−2752.
10. Hines, V., and Johnston, M. (1989) *Biochemistry 28*, 1227−1234.
11. Larsen, J. N., and Jensen, K. F. (1985) *Eur. J. Biochem. 151*, 59−65.
12. Andersen, P. S., Jansen, P. J. G., and Hammer, K. (1994) *J. Bacteriol. 176*, 3975−3982.
13. Rowland, P., Nielsen, F. S., Jensen, K. F., and Larsen, S. (1997) *Structure 5*, 239−252.
14. Rowland, P., Bjornberg, O., Nielsen, F., Jensen, K. F., and Larsen, S. (1998) *Protein Sci. 7*, 1269−1279.
15. Bjornberg, O., Rowland, P., Larsen, S., and Jensen, K. F. (1997) *Biochemistry 36*, 16197−16205.
16. Li, X., Weinstock, G. M., and Murray, B. E. (1995) *J. Bacteriol. 177*, 6866−6873.
17. Benkel, B. F., and Fong, Y. (1996) *Genet. Anal. 13*, 123−127.
18. Light, D. R., Walsh, C. T., and Marletta, M. A. (1980) *Anal. Biochem. 109*, 87−93.
19. Nielsen, F. S., Andersen, P. S., and Jensen, K. F. (1996) *J. Biol. Chem. 271*, 29359−29365.
20. Massey, V., Hofmann, T., and Palmer, G. (1962) *J. Biol. Chem. 237*, 3820−3828.
21. Copeland, R. A. (1994) *Methods for protein analysis*, pp 51−54, Chapman & Hall, New York and London.
22. Fibla, J., and Gonzalez, D. R. (1993) *J. Biochem. Biophys. Methods 26*, 87−93.
23. Orr, G. A., and Blanchard, J. S. (1994) *Anal. Biochem. 142*, 232−235.
24. Cleland, W. W. (1979) *Methods Enzymol. 63*, 103−138.
25. Vanoni, M. A., Wong, K. K., Ballou, D. P., and Blanchard J. S. (1990) *Biochemistry 29*, 5790−5796.
26. Batie, C. J., LaHaie, E., and Ballou, D. P. (1987) *J. Biol. Chem. 262*, 1510−1518.
27. Gassner, G., Wang, L., Batie, C., and Ballou, D. P. (1994) *Biochemistry 33*, 12184−12193.
28. Singer, T. P., Gutman, M., and Massey, V. (1973) in *Iron−sulfur proteins* (Lovenberg, W., Ed.) Vol. 1, pp 285−294, Academic Press, New York.
29. Jorns, M. S. (1985) *Biochemistry 24*, 3189−3194.
30. Massey, V., and Hemmerich, P. (1980) *Biochem. Soc. Trans. 8*, 246−257.
31. Vanoni, M. A., Edmondson, D. E., Zanetti, G., and Curti, B. (1992) *Biochemistry 31*, 4613−4623.
32. Megran, D. W. (1992) *Clin. Infect. Dis. 15*, 63−71.
33. Kahler, A. E., and Switzer, R. L. (1996) *J. Bacteriol. 178*, 5013−5016.
34. Podschun, B., Jahnke, K., Schnackerz, K., and Cook, P. (1993) *J. Biol. Chem. 268*, 3407−3413.
35. Porter, D. J. T., Chestnut, W. G., Taylor, L. C. E., Merrill, B. M., and Spector, T. (1991) *J. Biol. Chem. 266*, 19988−19994.
36. Rosenbaum, K., Jahnke, K., Schnackerz, K. D., and Cook, P. F. (1998) *Biochemistry 37*, 9156−9159.
37. Quinn, D. M., and Sutton, L. D. (1991) in *Enzyme mechanism from isotope effects* (Cook, P. F., Ed.) pp 73−123, CRC Press, Boca Raton.
38. Correll, C. C., Batie, C. J., Ballou, D. P., and Ludwig, M. L. (1992) *Science 258*, 1604−1610.
39. Karplus, A. P., Daniels, M. J., and Herriott, J. R. (1991) *Science 251*, 60−66.
40. Cleland, W. W. (1975) *Biochemistry 14*, 3220−3224.
41. Giard, J. C., Hartke, A., Flahaut, S., Boutibonnes, P., and Auffray, Y. (1997) *Res. Microbiol. 148*, 27−35.

BI990674Q